7

Light Sheet Microscopy

Gopi Shah[1,2], *Michael Weber*[1,3], *and Jan Huisken*[1,4]

[1] *Max Planck Institute of Molecular Cell Biology and Genetics, Pfotenhauerstr. 108, 01307 Dresden, Germany*
[2] *University of Cambridge, Cancer Research UK Cambridge Institute, Robinson Way, CB20RE Cambridge, UK*
[3] *Harvard Medical School, Department of Cell Biology, 200 Longwood Ave, LHRRB 113, Boston MA 02115, USA*
[4] *Morgridge Institute for Research, Department of Medical Engineering, 330 N Orchard Street, Madison WI 53715, USA*

Live imaging of whole tissues and organs is becoming increasingly important in modern-day biology. In recent years, light sheet microscopy, with its high speed and low phototoxicity, has become the technique of choice for long-term live imaging of developing organs and organisms. The earliest instrument to employ the principle of light sheet microscopy was the slit-ultramicroscope for counting gold particles in solution in 1902 [1]. Light sheet microscopy found its application for biology after the development of genetically encoded fluorescent proteins in the 1990s [2]. In 1993, a technique called orthogonal-plane fluorescence optical sectioning (OPFOS) used light sheet illumination to image the internal architecture of fixed cochlea [3]. However, it was not until 2004 that the application of light sheet microscopy was demonstrated for fast four-dimensional (4D) (x, y, z, t) live imaging of millimeter-sized embryos [4].

Every *in vivo* fluorescence microscope has a certain range of sample sizes where it performs best, with no single instrument that covers the entire range from subcellular resolution all the way up to whole embryos. On the small scale, confocal microscopy (Chapter 5) has been used to image tissue sections and parts of small model organisms at high resolution. On the large end of the scale, tomographic techniques have been established for reconstructing centimeter-sized samples at lower resolution. The gap between these technologies is now bridged by light sheet microscopy, which offers cellular resolution in millimeter-sized samples. Phototoxicity has been reduced to a minimum even at high acquisition rates, proving the technique most suitable for imaging developing embryos at high speed and very good resolution over several hours or days. In the last decade, light sheet microscopy has been successfully used to image dynamic processes in various model organisms: zebrafish [5, 6], Drosophila [4, 7, 8], *Caenorhabditis elegans* [9], spheroids [10], cell cultures as well as single cells [11–13]. At the same time, it has become the preferred technique for visualizing the structure of large specimens such as fixed and cleared brain and other organs in mouse [14]. It has also been used for imaging rapid processes such as the beating zebrafish

Fluorescence Microscopy: From Principles to Biological Applications, Second Edition.
Edited by Ulrich Kubitscheck.

heart and the blood flow [15, 16], as well as long-term slow events such as plant growth [17]. It is this versatile nature that makes light sheet microscopy a popular technology among cell and developmental biologists.

Although called by different names in the literature (selective plane illumination microscopy, SPIM, digitally scanned light sheet microscopy, DSLM, light sheet fluorescence microscopy, LSFM, ultramicroscopy, etc.), all implementations are based on the same fundamental principle described in this chapter. We will focus on the basics of the light sheet microscopy principle and construction, followed by an overview of its various implementations. In the end, we will discuss some of the novel data handling solutions that light sheet microscopy gave rise to, as well as future prospects in this area.

7.1 Principle of Light Sheet Microscopy

In light sheet microscopy, the sample is illuminated with a thin sheet of laser light to obtain optical sections. The microscope generally consists of two orthogonal optical axes: one for generating the light sheet for illumination, and the other for widefield detection of the emitted fluorescence. The two axes are aligned such that the illuminating light sheet is positioned in the focal plane of the detection unit (Figure 7.1).

As the specimen is illuminated with a sheet of laser light, the entire focal plane of the detection arm is illuminated providing instant optical sectioning as opposed to the slow point scanning used in confocal microscopy (Chapter 5).

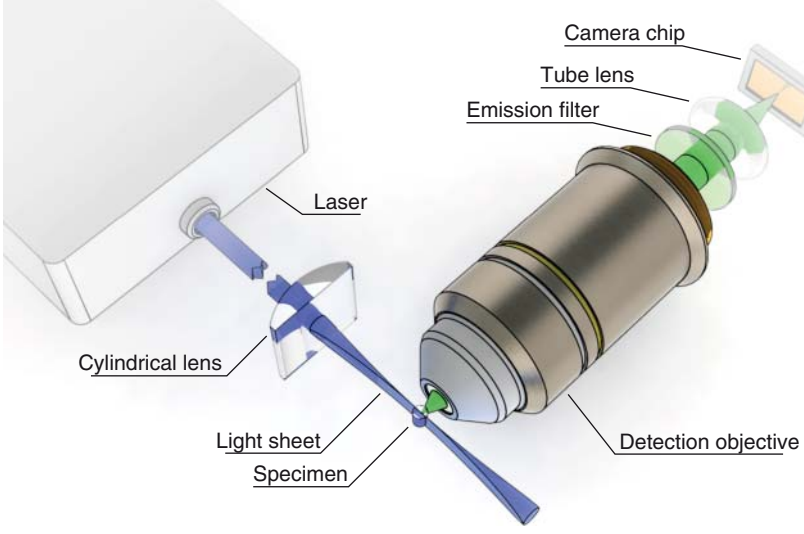

Figure 7.1 Principle of light sheet microscopy. Illumination and detection axes are oriented orthogonally, and the specimen is placed at their intersection. A sheet of laser light is produced, for example, using a cylindrical lens, and illuminates a thin slice of the sample in the focal plane of the detection objective. A camera, which is placed behind the detection lens, the fluorescence filter, and the tube lens, captures an image of the fluorescence.

The height and thickness of the light sheet can be adjusted to achieve the desired extent of optical sectioning and to illuminate the entire field of view (FOV). Fluorescence generated by the light sheet is collected very efficiently, as all the camera's pixels collect photons simultaneously during the entire exposure time. By using fast and sensitive cameras, the sample is imaged rapidly with low light exposure. Therefore, light sheet microscopy is an ideal technique to capture dynamic developmental processes without detrimental phototoxicity and to image large, cleared organs fast and efficiently.

Theoretically, a light sheet microscope's lateral resolution is equivalent to that of an epi-fluorescence microscope (with the same objective lens), given by the objective lens' numerical aperture (NA) and the fluorophore's wavelength λ_{em} (Chapter 2, Section 2.3.4). In practice, however, the contrast in light sheet microscopy is generally better because of the optical sectioning. The depth of the optical section is defined by the thickness of the light sheet. As a consequence, high axial resolution can be obtained even with low-NA, low-magnification detection lenses, which usually have a large working distance desirable for large sample imaging.

7.2 Light Sheet Microscopy: Key Advantages

Light sheet microscopy offers several advantages over conventional imaging modalities. The main reason for the success of light sheet microscopy in the biological sciences is certainly the heavily reduced phototoxicity. Traditional compound and confocal microscopes illuminate the entire volume of the sample, even when imaging only a single plane. Even worse, when a z-stack of N images is recorded, the entire sample is exposed to the excitation light N times. In contrast, in light sheet microscopy one image plane at a time is illuminated. Therefore, during a stack across the entire sample, every plane is exposed only once, minimizing the risk of photobleaching and phototoxicity.

In point scanning microscopes, each point is sequentially exposed and detected, requiring higher laser power and typical exposure times of several seconds to obtain a single image. In light sheet microscopy, the entire plane is illuminated simultaneously, and photons from the entire field of view are collected in parallel within an exposure time of a few milliseconds. This exposure time is about a thousand times longer than the pixel dwell time in a point scanning system, which is in the range of a few microseconds per pixel. Using fast and sensitive EM-CCD and scientific complementary metal-oxide-semiconductor (sCMOS) cameras, one can rapidly acquire images with excellent dynamic range and signal-to-noise ratio. Fluorophore saturation, unlike in confocal point scanning microscopy, is less of an issue in light sheet microscopy. The acquisition speed is limited only by the camera technology and available fluorescence signal and can be exploited in a number of ways. Most importantly, one can study very fast three-dimensional phenomena that are too complex to reconstruct with conventional widefield microscopy and too fast for confocal microscopy [15, 18].

The fast recoding in light sheet microscopy is also another key advantage for the imaging of large scattering objects. The ability to record an entire z-stack in

a few seconds opens up the possibility to record additional views of the sample from other directions. The classical horizontal setup of the objective lenses is particularly well suited for this multiview imaging: since the sample hangs vertically at the intersection of the two optical axes, it can be rotated without deformation. While other imaging modalities are simply too slow, several views can be obtained within a few seconds on a light sheet microscope and fused to reconstruct the whole sample without artifacts [19]. Two orthogonal or more views are merged for improving the axial resolution, for example, by multiview deconvolution, or to simply increase the overall information content of the volume when imaging large specimen that cannot be optically penetrated from a single side [20–22].

Furthermore, the orthogonal geometry provides flexibility to tweak the illumination and the detection arms independently to adapt to the experimental needs. Consequently, there are several technical implementations of light sheet microscopy developed for a wide range of applications discussed later in this chapter.

7.3 Construction and Working of a Light Sheet Microscope

Two different ways of generating a light sheet are commonly used: in SPIM, the laser beam is expanded and focused using a cylindrical lens to form the sheet of light (Figure 7.2a) [4]. This method is simple to implement and widely used for fast and gentle low-light *in vivo* applications. Alternatively, a "virtual" light sheet can be generated by the DSLM technique, which uses a scanning mirror to rapidly sweep a beam across the FOV (Figure 7.2b) [5]. This method offers more flexibility, as the height of the light sheet can be easily adapted by changing the scanning amplitude, and its thickness by changing the diameter of the incoming laser beam. Here, because of the sequential line illumination, only a fraction of the final image is illuminated at a given point in time, exposing the sample to a local light intensity much higher than in SPIM in order to achieve the same fluorescence yield in the same amount of time. While this may result in fluorophore saturation and higher photobleaching, it is compatible with applications that require high laser power such as two-photon excitation [23], beam-shaping applications like Bessel beam illumination [12, 24], and structured illumination [25].

In DSLM, the light sheet has a uniform intensity profile along its height, whereas in SPIM the laser light is expanded and cropped with apertures to cover the FOV of the detection lens, resulting in a less uniform intensity profile. However, the simultaneous plane illumination obtained in SPIM is preferred for high-speed imaging applications, especially when using electrically tunable lenses (ETLs) and ultrafast cameras for image acquisition without motion artifacts. Therefore, when designing a light sheet microscope, it is crucial to determine the application for which it will be used in order to choose the appropriate means to produce the light sheet. The following section presents a detailed overview of designing a light sheet microscope setup with a static light sheet.

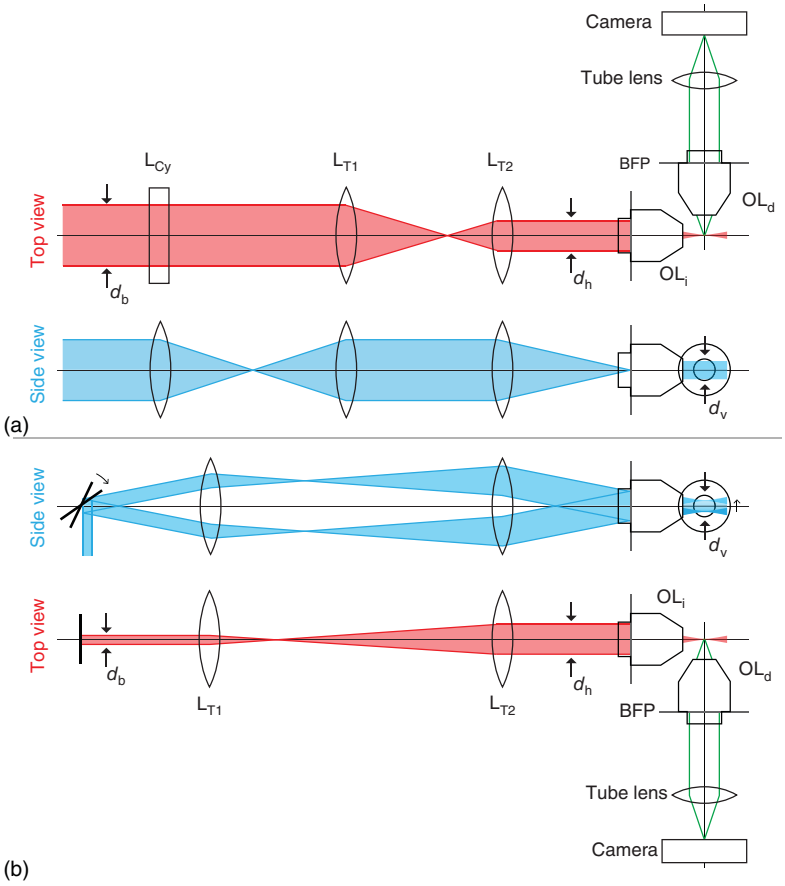

Figure 7.2 Beam paths of microscopes with static and scanned light sheet illumination. (a) Static light sheet illumination. An incoming laser beam of diameter d_b passes a cylindrical lens L_{Cy} and is focused to a line. A telescope comprising the lenses L_{T1} and L_{T2} adapts the beam height d_h and focuses it into the back focal plane (BFP) of the illumination objective OL_i, which projects a light sheet into the focal plane of the detection objective OL_d. The excited fluorescence signal is collected by OL_d and focused onto a camera by means of a tube lens. (b) Scanned light sheet illumination. The major difference from a microscope with static light sheet illumination is an incoming laser beam that is rapidly scanned along one axis in the BFP of L_{T1}, resulting in a sweeping laser beam that generates a "virtual" light sheet in the focal plane of OL_d.

7.4 Theory of Light Sheet Microscopy

A light sheet can be easily generated with a single cylindrical lens. Its focal length and the incoming beam diameter determine the thickness and extent of the light sheet. While this simple setup may be sufficient to generate a single-colored sheet in air, it does not fulfill the requirements in biological imaging. For example, it is desirable to generate several overlapping light sheets with different wavelengths and to work in an immersion medium such as water. It is therefore advisable to use

a well-corrected objective lens, specifically designed for the desired immersion medium. Hence, many SPIM setups feature not only a water-dipping detection lens but also a matching water-dipping illumination lens. The optics need to be designed in such a way that the last element is an objective lens; the cylindrical lens is placed earlier in the beam path. In addition, it is desirable to have enough degrees of freedom to adjust the position, orientation, and thickness of the light sheet. Therefore, mirrors and slits are inserted wherever appropriate. Here, we will go through calculations that enable us to pick the right parts for designing a SPIM setup that features a cylindrical lens and an objective lens for light sheet formation.

The light path of the illumination arm consists of a laser and a beam expander, optionally a fiber and a collimator. The collimated beam is sent onto a cylindrical lens L_{Cy} to generate a light sheet, which is then imaged into the back focal plane (BFP) of the illumination objective lens. In order to get a vertical light sheet at the sample, the sheet in the BFP needs to be horizontal. Ideally, a mirror is placed in the BFP to allow precise positioning of the sheet (in order to place it in the focal plane of the detection plane). Since the BFP of the illumination lens is usually inside the housing of the lens and therefore not accessible, one uses a telescope of two lenses to image the back focal plane onto a mirror. This arrangement gives access not only to the BFP but also to the focal plane of the illumination lens. With mirrors and slits, the dimensions and position of the beam can be easily adjusted. The following considerations are important to obtain a light sheet that is thin yet uniform across the entire FOV. We consider a set of four lenses to form the light sheet in the sample chamber: a cylindrical lens L_{Cy}, two lenses L_{T1} and L_{T2}, and an objective lens OL_i. Further we assume a Gaussian beam of diameter d_b to hit L_{Cy} (Figure 7.2). The light sheet in the sample chamber has a shape as depicted in Figure 7.3. The beam converges to a waist of $2\omega_0$ and diverges again.

A convenient measure of the extent of the light sheet is given by the Rayleigh length x_R, which is defined as the distance from the waist to the plane where the beam has expanded to $\sqrt{2}\,\omega_0$, that is,

$$\omega(x_R) = \sqrt{2}\,\omega_0.$$

The Rayleigh length is given by

$$x_R = \frac{\pi n \omega_0^2}{\lambda} \quad \text{or} \quad \omega_0 = \sqrt{\frac{x_R \lambda}{\pi n}} \tag{7.1}$$

where ω_0 is half the thickness at the waist of the light sheet, λ is the wavelength of the beam, and n is the refractive index of the medium. We can further approximate (see Figure 7.3)

$$\phi/2 \approx \tan(\phi/2) = \frac{d_{BFP}/2}{f_{IO}} \quad \text{or} \quad \phi \approx \frac{d_{BFP}}{f_{IO}} \tag{7.2}$$

where f_{IO} is the focal length of the illumination objective and d_{BFP} is the width of the beam in the BFP of the objective lens. The total angular spread of a Gaussian beam in radians is related to the beam waist ω_0 by

$$\phi = \frac{2\lambda}{\pi n \omega_0} \tag{7.3}$$

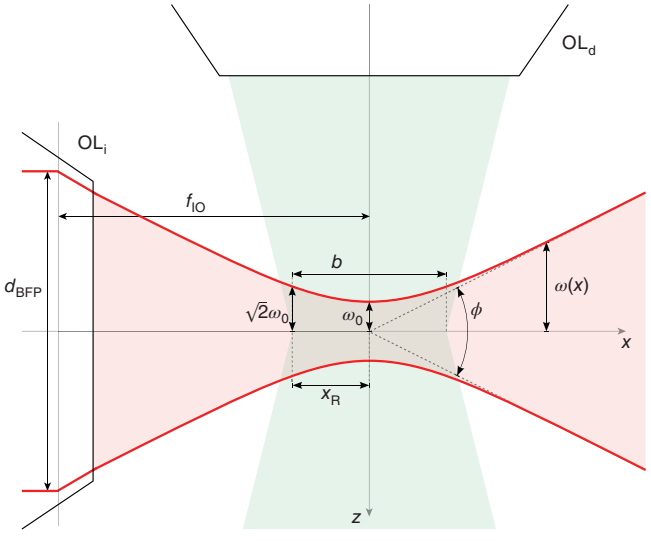

Figure 7.3 Relationship between light sheet dimensions and field of view. A light sheet is generated from a laser with Gaussian beam width $\omega(x)$ and total angular spread (ϕ). The waist of the light sheet is placed in the middle of the field of view and its properties are adjusted such that the distance (2× Rayleigh length x_R) equals the width of the field of view.

From Eqs (7.2) and (7.3), we get

$$\frac{d_{\mathrm{BFP}}}{f_{\mathrm{IO}}} = \frac{2\lambda}{\pi n \omega_0}.$$

Substituting the value for ω_0 from Eq. (7.1), we have

$$d_{\mathrm{BFP}} = \frac{2\lambda f_{\mathrm{IO}}}{\pi n}\sqrt{\frac{\pi n}{x_{\mathrm{R}}\lambda}} = 2f_{\mathrm{IO}}\sqrt{\frac{\lambda}{\pi n x_{\mathrm{R}}}}. \tag{7.4}$$

From this equation, we can calculate how wide our beam needs to be at the BFP of our illumination lens d_{BFP} in order to get a sheet with a length of x_{R}. The width of the FOV (along x-axis) should be equal to $2x_{\mathrm{R}}$, and d_{BFP} can be calculated. In other words, x_{R} can be expressed as

$$2x_{\mathrm{R}} = \frac{N_x^{\mathrm{px}} d^{\mathrm{px}}}{M_{\mathrm{DO}}} \tag{7.5}$$

where N_x^{px} is the number of pixels along the x-axis, d^{px} is the pixel size, and M_{DO} is the magnification of the detection objective.

From the top view of the light path in Figure 7.2, d_{BFP} can be expressed as

$$d_{\mathrm{BFP}} = d_{\mathrm{b}}\frac{f_{\mathrm{T2}}}{f_{\mathrm{T1}}} = d_{\mathrm{b}}M_{\mathrm{T}} \qquad \text{or} \qquad d_{\mathrm{b}} = \frac{d_{\mathrm{BFP}}}{M_{\mathrm{T}}} \tag{7.6}$$

where d_{b} is the diameter of the incoming circular beam, M_{T} is the magnification, and f_{T1},f_{T2} are the focal lengths of the telescope in front of the illumination lens. At the same time, from the side view of the light path in Figure 7.2, the height of

the light sheet can be expressed as

$$d_h = \alpha_y d_b \frac{f_{T1}}{f_{Cy}} \frac{f_{IO}}{f_{T2}} = \alpha_y d_b \frac{1}{M_T} \frac{f_{IO}}{f_{Cy}} \quad \text{or} \quad d_b = \frac{d_h M_T f_{Cy}}{\alpha_y f_{IO}} \tag{7.7}$$

where f_{Cy} is the focal length of the cylindrical lens. We have introduced the factor α_y, which describes how much the beam is cropped in order to achieve an almost uniform intensity distribution across the height of the beam. In the instrument, an iris or a slit is introduced to cut off the tails of the Gaussian beam. Similarly, a factor α_z may be introduced to describe the cropping of the beam horizontally (along z) to adjust the light sheet thickness (cropping the beam horizontally will make the light sheet wider and longer). α ranges from 1 (fully open) to 0 (fully closed).

From Eqs (7.6) and (7.7), we can write

$$\frac{d_{BFP}}{M_T} = \frac{d_h M_T f_{Cy}}{\alpha_y f_{IO}} \quad \text{or} \quad M_T = \sqrt{\frac{d_{BFP} f_{IO} \alpha_y}{d_h f_{Cy}}} \tag{7.8}$$

d_h is the height of the desired FOV, therefore the magnification of the telescope M_T can now be determined, by inserting the value for d_{BFP} from Eq. (7.4). The incoming beam diameter d_b can be obtained, and an appropriate beam expander or collimator can be included to obtain the desired diameter.

In the case of DSLM, the height of the light sheet is regulated by the scanning amplitude and the thickness by the diameter of the incoming beam. While the light path does not contain a cylindrical lens (Figure 7.2b), the remaining calculations are identical for both SPIM and DSLM.

Example 1: System Design for Imaging an Early Zebrafish Embryo that Fits Entirely in an 800 × 800 µm FOV

We know

- width of the FOV: $2x_R = 800$ µm $= 0.8$ mm
- height of the FOV (and light sheet): $d_h = 800$ µm $= 0.8$ mm
- wavelength of illumination $\lambda = 0.488$ µm
- refractive index of medium $n = 1.33$
- illumination objective: 10×, $f_{IO} = 19$ mm
- focal length of cylindrical lens commonly used $f_{Cy} = 50$ mm
- slit $\alpha_y = 0.25$.

Substituting values in Eq. (7.4), the beam diameter in the BFP of the illumination objective should be $d_{BFP} = 0.649$ mm. Substituting values in Eq. (7.8), the required magnification of the telescope is obtained as $M_T = 0.278$. Therefore, the lenses T1 and T2 need to be chosen such that $f_{T2}/f_{T1} = 0.278$.

From Eq. (7.6), the required incoming beam diameter d_b should be at least 2.34 mm. Using these components, the resulting light sheet thickness can be calculated from Eq. (7.2) to be $2\omega_0 = 13.7$ µm.

As the FOV here is quite large, the light sheet is relatively thick at its waist. In the next example, we will look at a smaller FOV and see how the light sheet thickness and beam diameter in the BFP change.

Example 2: System Design for Imaging a Drosophila Embryo, Which Would Require 300 × 500 µm FOV

We use the same parameters as before, except for the following:

- width of the FOV: $2x_R = 300\ \mu m = 0.3\ mm$
- height of the FOV (and light sheet): $d_h = 500\ \mu m = 0.5\ mm$.

Substituting values in Eq. (7.4), the beam diameter in the BFP of the illumination objective should be $d_{BFP} = 1.06$ mm. Substituting the values in Eq. (7.8), the required magnification of the telescope is obtained as $M_T = 0.449$.

Therefore, from Eq. (7.6), the required incoming beam diameter d_b should be at least 2.36 mm. Using these components, the resulting light sheet thickness can be calculated from Eq. (7.2) to be $2\omega_0 = 8.37\ \mu m$.

7.5 Light Sheet Interaction with Tissue

All light microscopes suffer from artifacts by the interaction of the light with the sample. Scattering and attenuation of excitation and emission light are major issues. While traveling through dense tissue, the excitation light is attenuated and scattered: scattering within the plane of the light sheet is not a problem, but scattering along the z-axis leads to an increase in light sheet thickness and loss of z-sectioning (Figure 7.4a). Choosing the right polarization of the light sheet is crucial to minimize this effect: the laser beams in light sheet microscopy are polarized, and the scattering in tissue is polarization dependent. This effect can be easily observed by using a $\lambda/2$-plate to rotate the polarization. Turning the polarization and maximizing the scattering within the plane, that is, toward an observer looking at a SPIM chamber from the top, yields the correct polarization.

Attenuation of the excitation light and the emitted fluorescence results in stripy and patchy images. Especially in large samples, the part of the sample facing the incoming light sheet yields better contrast and signal-to-noise ratio, as the signal degrades going deeper into the sample (Figure 7.4a). To overcome this issue, the sample can be illuminated from two opposite sides, obtaining good image quality in both halves of the sample (Figure 7.4b). It is important to note that the double-sided illumination is ideally performed sequentially, recording one image for each illumination. The two images are merged either directly or later during post-processing. Thereby, the aberration-free parts facing the illumination are preserved and contribute to the final image. Illumination from both sides simultaneously is advisable only when the sample is sufficiently transparent and the

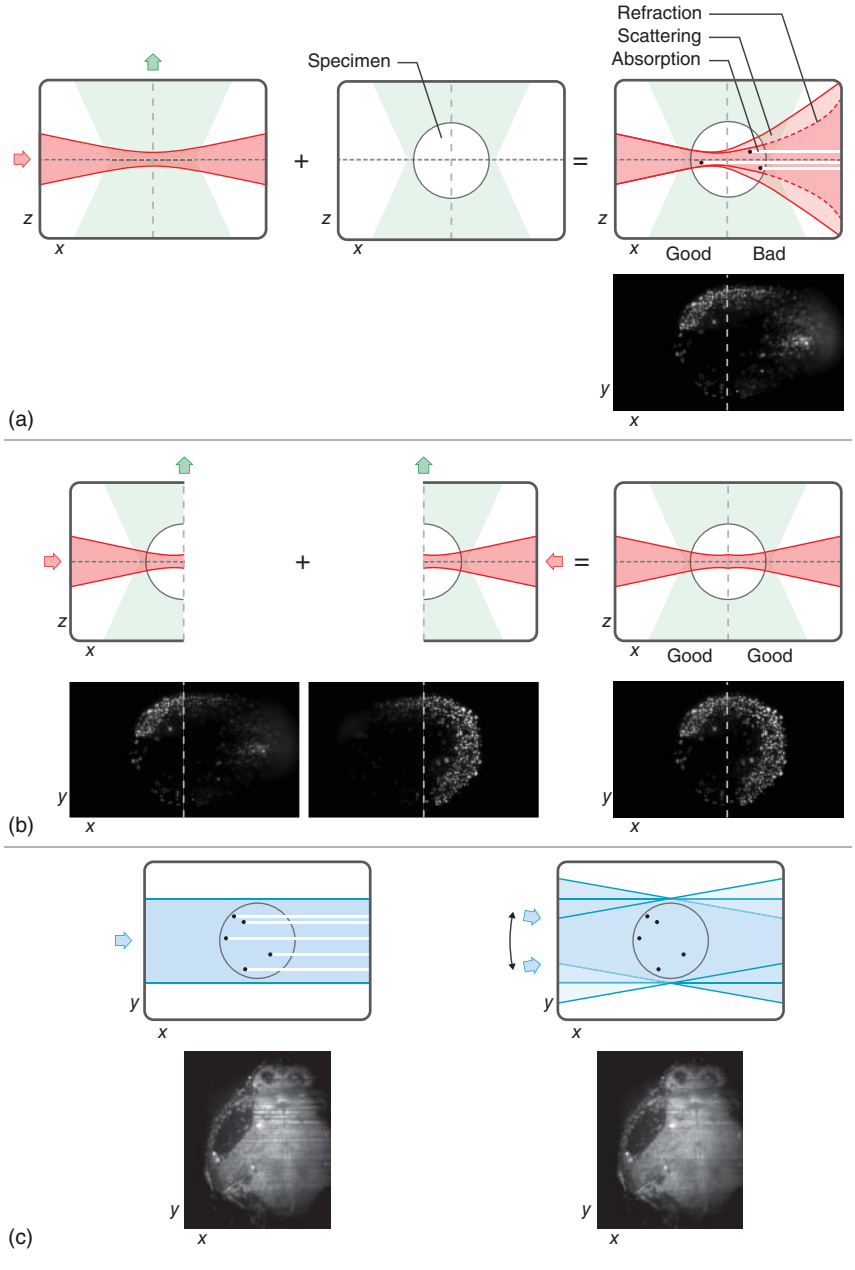

Figure 7.4 Correction of sample-induced effects on the light sheet. (a) Single-sided illumination. (b) Double-sided illumination. (c) Pivoting light sheet. Obstacles in the field of view potentially result in stripes along the propagation direction of the light sheet illumination. By using a light sheet that pivots around the center of the field of view within one exposure, the propagation direction is constantly altered. Thereby, obstacles are homogeneously illuminated from a range of angles, and the sum of the excited fluorescence results in an image with a minimum number of visible stripes.

scattered thicker light sheet from one side does not deteriorate the other thinner light sheet.

The absorption of the excitation light produces artifacts such as stripes of bright and shadowed regions across the entire FOV (Figure 7.4c). In light sheet microscopy, this effect is especially pronounced and visible as a result of the illumination from the side. To overcome this problem, multidirectional SPIM (mSPIM) has been developed [26], which includes a combination of double-sided sequential illumination and light sheet pivoting. More even illumination of the FOV is achieved by pivoting the light sheet, that is, scanning the beam over an angle of ca. 10 deg at a frequency of about 1 kHz with a resonant mirror during a single exposure of the camera. By doing so, the stripes and shadows in the image are greatly reduced, thereby achieving a more homogenous image quality across the whole sample (Figure 7.4c).

7.6 3D Imaging

So far we have discussed how to acquire 2D images of a sample using light sheet microscopy. However, most biological applications require 3D imaging. Given its excellent optical sectioning capability, speed, and low phototoxicity, light sheet microscopy is ideally suited for fast 3D imaging. For a variety of samples, different modes of 3D image acquisition have been developed.

I. A widely used approach is to acquire a *z*-stack by translating the sample along the detection axis, through a static light sheet, as the camera continuously records images (Figure 7.5a). Only the sample is moved, and the rest of the

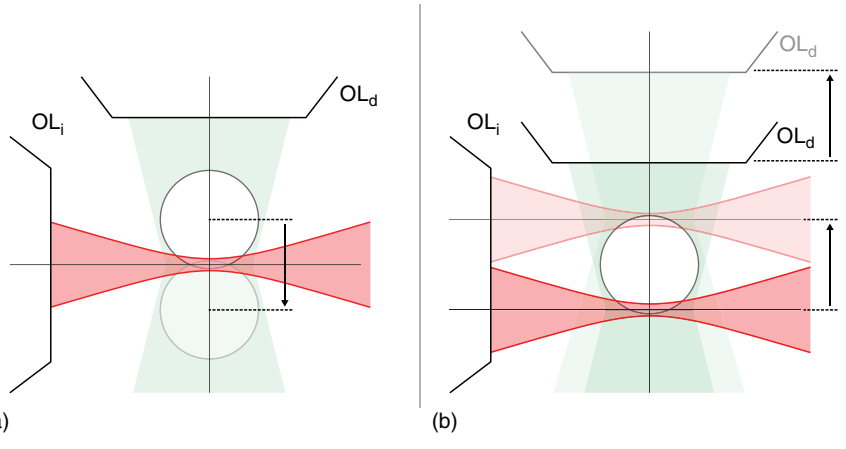

Figure 7.5 Two strategies to record *z*-stacks in a light sheet microscope. (a) Translating the sample. The specimen is moved through the static focal plane of the detection objective OL_d, which is continuously illuminated with a light sheet. (b) Translating illumination and detection. The focal plane is moved through the static specimen, for example, by translating OL_d. Simultaneously, a scan mirror maintains a light sheet in the focal plane of OL_d.

optics remains fixed. This method ensures that the light sheet stays in the focal plane of the detection lens after alignment of the system, making it robust and straightforward to implement. Moving the sample continuously rather than stepwise ensures fast and smooth data acquisition with minimum artifacts. The illumination time of the sample needs to be kept short, or the motors need to move slowly, to minimize bluring and thickening of the light sheet as the sample is moved during the exposure. The imaging speed is ultimately limited by the speed of the motors and the speed at which a given sample can be moved without affecting its physiology.

II. A more recent approach is to keep the sample static while scanning the light sheet through it. A major advantage of such a system is that it is independent of the sample, and even fragile samples can be imaged contactless. Such a system is especially beneficial for imaging samples that cannot be embedded in a solid medium such as agarose, and need to be in a water-like medium for their proper growth and movement. However, when continuously moving the light sheet, the focal plane of the detection system needs to be synchronized with the light sheet movement to keep the fluorescence in focus. Alternatively, one could also expand the depth of focus to cover the entire scan range, which generally requires deconvolution or sacrificing lateral resolution. The two main remote focusing approaches are as follows:
   a) Using a motorized objective lens: In such a system, fast and precise short-range stages or piezo-driven stages are used to rapidly move the objective lens back and forth. When synchronized with a galvanometric mirror used to scan the light sheet, fast *z*-stacks can be obtained without moving the sample (Figure 7.5b). While many light sheet microscopes use water-dipping objective lenses, air lenses are better suited for this setup to prevent any leakage from the sample chamber and avoid pressure waves in the medium. Nevertheless, the use of motorized water-dipping lenses has been demonstrated for brain and whole-animal imaging of Drosophila larvae [27]. An alternate approach had been developed earlier to image neurons, wherein an optical fiber producing a light sheet was mechanically coupled to the moving detection lens to ensure the synchronized movement of the light sheet with respect to the detection objective lens [28].
   b) Using an ETL: An ETL is a liquid-filled, deformable lens that changes its curvature in response to an electrical signal, resulting in a change of its focal length and a shift of the focal plane (Figure 7.6). Rapid *z*-stacks are acquired by moving the light sheet and refocusing the detection optics remotely by modulating the current in the ETL [29]. Here, the depth of the stack is proportional to the focusing range of the ETL. Large volume scanning at moderate speed can be obtained. Ultimately, the speed of such a system is limited by the fluorescence yield; cameras with 10 000 frames per second are available and principally applicable to achieve hundreds of volumes per second. High-speed scanning of smaller volumes, necessary for imaging highly dynamic processes, such as a beating zebrafish heart and blood flow, have been demonstrated with a fast CMOS camera [15].

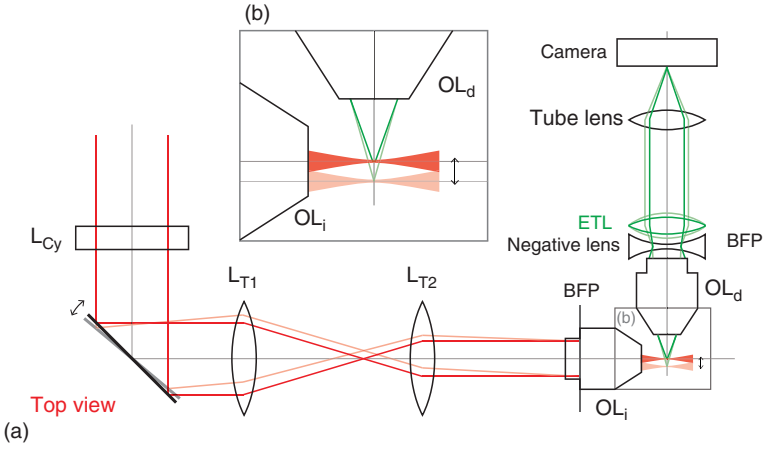

Figure 7.6 Beam path of a light sheet microscope with an electrical tunable lens (ETL). (a) An ETL in the microscope's detection path oscillates the focal plane of the detection objective OL_d along the detection axis, *z*. A scan mirror simultaneously maintains a light sheet in the focal plane of OL_d. (b) The intersection of illumination and detection axes with the oscillating focal plane and the scanned light sheet.

7.7 Multiview Imaging

The penetration depth of a light microscope is limited by attenuation and scattering of excitation and emission light. Thus, images recorded in areas facing the illumination and detection objectives provide better contrast and signal-to-noise ratio than those acquired in deeper regions. It would therefore be advantageous if the arrangement of the sample with respect to illumination and detection axes could be adapted. In a light sheet microscope, *z*-stacks can be obtained from different viewing angles by rotating the sample. Importantly, this is not necessarily a unique feature of light sheet microscopy. However, a prerequisite for successful multiview imaging in living samples is high acquisition speed. Multiple views need to be acquired in quick succession to avoid developmental changes in the sample, making the datasets incompatible. Multiple views of the sample are then fused to reconstruct the entire sample in three dimensions (Figure 7.7a). This method provides two major advantages: multidirectional illumination and detection of entire samples, resulting in increased image quality and information content throughout the sample. Moreover, different views of the same area of the sample can be fused to improve the axial resolution of the data: for example, ideally the poor axial resolution of one dataset is replaced by the good lateral resolution of a dataset recorded perpendicular to the first.

Several computational methods have been developed to merge *z*-stacks recorded from multiple viewing angles. Precise registration of the datasets is crucial for successful fusion. Ideally, the micromotors and rotational motors used to orient and position the sample are precise and reproducible so that an initial calibration is sufficient to register subsequent datasets. Otherwise, fluorescent beads need to be added as fiducial markers, or nuclear markers

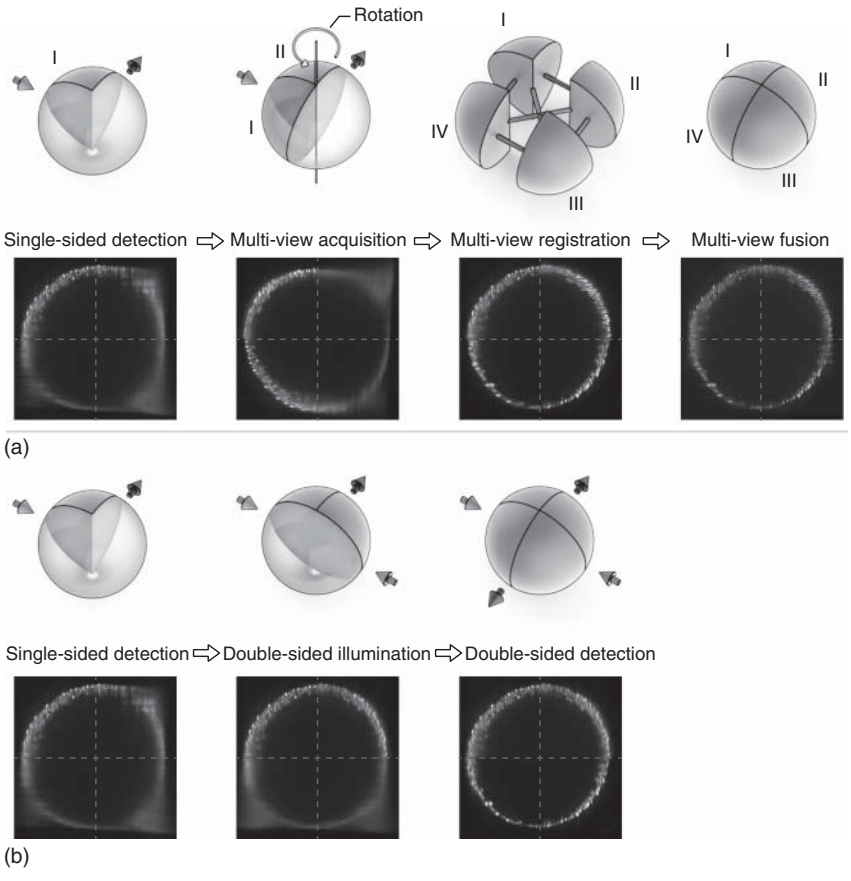

Figure 7.7 Multiview acquisition strategies. (a) Stepwise rotation of the sample. A specimen is rotated around its center in steps of, for example, 90 °, and *z*-stacks are acquired from each angle (multiview acquisition). Single-sided illumination and detection result in about 25% coverage of the sample. Multiview registration and fusion combines the well-covered areas of each recording into a homogeneous dataset. (b) Multi-sided detection of a static sample. The limited coverage of single-sided illumination and detection is overcome by illuminating the specimen from two sides (double-sided illumination) while recording consecutive *z*-stacks from two sides (double-sided detection).

inside the sample can serve as landmarks to register the different views to each other. These reference points in different views are matched with each other to determine the transformation between adjacent views. The different views are then fused accordingly to obtain a 3D reconstruction of the entire sample (Figure 7.7a). Deconvolution based on point spread functions recorded from multiple views can also be used to improve the axial resolution and contrast of images [21]. Real-time deconvolution by re-slicing the acquired data and processing cross-sectional planes individually on the graphics processing unit (GPU) has been demonstrated and offers the efficient application of multiview acquisitions also in extended time lapse experiments [22]. An alternate and efficient method is to selectively acquire the well-resolved parts from each view

(quadrants that are well illuminated and detected) and stitch the "good" parts together to reconstruct the entire embryo with good signal-to-noise ratio [6]. Oftentimes, it is not clear at the beginning of a timelapse recording which view may yield the best data. Multiview acquisitions can then be performed to defer the decision and simply delete inferior data after acquisition.

7.8 Different Lens Configurations

A typical two-lens SPIM setup consists of an illumination and a detection arm, with a water-filled sample chamber at their intersection (Figure 7.8a). Water-dipping lenses are preferred, as they minimize the number of interfaces for illumination and detection; however, the orthogonal arrangement of illumination and detection objectives limits the choice of lenses. Often, high-NA

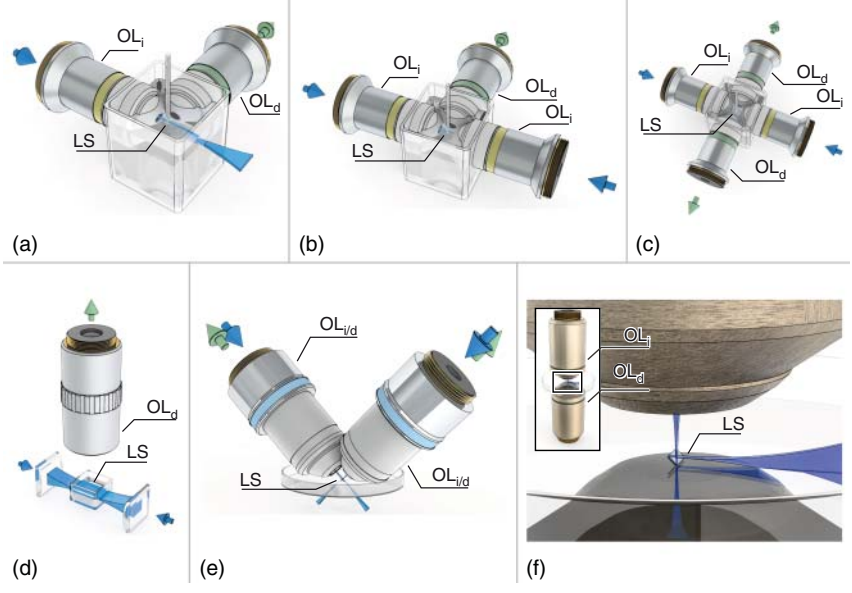

Figure 7.8 Diverse light sheet microscope designs. (a) A two-lens selective plane illumination microscope (SPIM) features single-sided illumination and detection and typically requires a vertically mounted sample. (b) In a three-lens or multidirectional SPIM (mSPIM), a second illumination path generates and additional light sheet to illuminate the sample simultaneously or alternately from two sides (double-sided detection). (c) A four-lens SPIM adds a second detection path to simultaneously or successively record images from two opposite sides. (d) Ultramicroscopes are typically designed around larger samples and facilitate a low-magnification objective in an upright detection path. The sample is illuminated with horizontally oriented light sheets from one or two sides. (e) The dual inverted SPIM (diSPIM) is an adaption of a two-lens configuration to accommodate specimens mounted in conventional dishes or multiwell plates. To provide a level of multiview imaging, illumination and detection can be alternated between the two objectives. (f) Reflected light sheet microscopy describes setups in which the orthogonal light sheet illumination is provided by reflecting the beam next to the specimen by means of a small mirror.

detection objectives are too big to be combined with an orthogonally placed water-dipping illumination objective. Therefore, in many cases, air illumination objectives need to be used. Fortunately, low NA illumination objectives such as 10×/0.3 lenses are sufficient to generate a light sheet with a thickness of only a few micrometers.

One of the beauties of light sheet microscopy is the flexibility of its design and the ease with which it can be customized for desired applications. Recent years have seen several implementations for imaging samples from single cells to multicellular vertebrate embryos, and developmental processes ranging from a plant growing over days to a zebrafish heart beating several times a second. The orthogonal optical arrangement of the illumination and detection paths can be set up horizontally for imaging most samples (Figure 7.8a). In a three-lens SPIM, a second identical illumination arm illuminates the sample from the opposite side (Figure 7.8b) [26]. The design of light sheet microscopes inspired the concept of multiview imaging. At the same time, the need for multiview imaging of large biological samples has inspired more advanced implementations of light sheet microscopy. Adding a second detection lens such that both light sheets are aligned with the shared focal plane of the two detection lenses gives two opposite views of the sample simultaneously (Figures 7.7b and 7.8c) [6–8].

A vertical configuration may be preferred for brain imaging [30] and imaging of cleared tissues when the sample is mounted horizontally such as in ultramicroscopy (Figure 7.8d) [14] or in single-molecule tracking [31]. For cells in culture or any sample that needs to be mounted on a coverslip, an inverted configuration like the diSPIM (Figure 7.8e) [9] or the reflected light sheet microscope, where a light beam is reflected from a scanning mirror to image through the same or oppositely placed detection lens, is more appropriate (Figure 7.8f) [32].

7.9 Sample Mounting

As is also true for other fields of light microscopy, sample mounting for light sheet microscopy has to fulfill two major tasks. The first one is to keep the specimen stable over the course of the recording to avoid blur and distortions. The second task is to minimize light attenuation and scattering, and maximizing resolution and contrast by using refractive index-matched and optically clear mounting materials. If living samples are examined, an additional task for sample mounting is to ensure the best possible conditions for the unaffected survival and well-being of the specimen over the course of the experiment.

The large variety of specimens imaged with light sheet microscopy, as well as the multitude of light sheet microscope designs, requires entirely different sample mounting strategies. Crucially, whether the specimen is alive or fixed (and potentially optically cleared) determines how to embed it. In case of living samples, such as fruit fly or zebrafish embryos, cultured tissue or cells, the mounting materials are typically matched to the refractive index of water (1.33). A frequently used strategy is to embed the specimen in a solid or viscous gel such as agarose, phytogel, or methylcellulose. If the specimens are fixed, mounting materials with

higher refractive indices are ideal (1.4–1.5). The optional use of clearing solutions increases the transparency of thicker fixed samples, but also has an impact on the refractive index [33, 34]. Some of those solutions are harmful and must not come into contact with optics (or the user), which requires an enclosed sample chamber and air lenses.

Sample mounting for light sheet microscopy goes hand in hand with the respective technical implementation. A requirement in all designs is the access from at least two orthogonal directions: the illumination and the detection axes. Some light sheet microscopes resemble traditional compound microscopes by using common microscope bodies (iSPIM) [9] and some of them even by using the same objective for illumination and detection (reflected light sheet microscopy, swept confocally-aligned planar excitation microscopy) [32, 35]. This permits the use of established protocols such as mounting the specimen in a Petri dish. However, the design of many light sheet microscopes is inspired by the early horizontal design, which differs significantly from that of common compound microscopes [4]. Having the specimen hanging inside a medium-filled chamber required rethinking, and initiated the development of novel mounting strategies to accommodate a variety of specimen. Widely used were gel columns made from agarose or phytogel [17, 36], or medium-filled polymer tubes or bags [37]. Many of these protocols do not simply reproduce existing techniques, but rather enable new types of experiments. When embedded in an agarose column or polymer tube, the specimen can be imaged from the best possible angle [15] or reconstructed from multiple angles [6]. Dedicated mounting protocols also enable light sheet microscopy of cell cultures, spheroids and organoids [38], as well as developing plants [17].

7.10 Recent Advances in Light Sheet Microscopy

Despite the fast multiview capabilities of SPIM, it still remains challenging to image millimeter-sized embryos fast and efficiently. Internal organs like the pancreas, liver, and gut in the zebrafish have been difficult to resolve with satisfactory resolution. Custom microscope setups that are tailored to the specific needs of the experiment and provide better penetration without additional phototoxicity are now needed.

A number of methods have been developed to suppress the scattered light in DSLM. While this makes the images crisper, it eliminates information, albeit blurry. The most popular solution is to use the rolling shutter of an sCMOS camera [39]. In this mode, the beam's position on the chip is synchronized with the rolling shutter of the camera. By selecting the correct "slit" width, scattered light can be eliminated.

Several attempts have been made in recent years to increase the penetration of DSLM. Two-photon excitation had been successfully applied in confocal scanning microscopy to increase penetration. The nonlinearity of the excitation permits eliminating the pinhole, the major bottleneck in deep-tissue imaging in confocal microscopy. In addition, the longer excitation wavelength scatters less and penetrates deeper into optically dense tissue. Hence, the implementation of

two-photon light sheet microscopy was straightforward in a DSLM system [23]. While providing improved penetration, serious issues have been the low excitation efficiency and the abrupt loss in excitation as soon as the light sheet gets scattered and widened, making quantitative analysis difficult. In addition, the potentially increased phototoxicity needs to be carefully evaluated.

DSLM also offers the opportunity to modify the beam modes and explore alternative profiles such as Bessel or Airy beams. The Bessel beam offers a long, thin core and would be ideally suited for the generation of thin and long light sheets. In addition, the beam is relatively robust against scattering [24, 40]. Unfortunately, the Bessel beam's thin core is accompanied by a set of rings that cause a lot of unwanted out-of-focus excitation. Suppression of these by confocal slit detection and two-photon excitation has been demonstrated. By generating a linear array of Bessel beams and making them to interfere, the rings can be eliminated and an optical lattice is generated (lattice light sheet microscopy [41]). Such ultrathin light sheets are particularly suited for imaging single cells.

Fluorescence is a prerequisite for light sheet microscopy and provides selective staining of distinct tissues. In many not-so-well-established model organisms, the absence of transgenic tools often limits *in vivo* imaging studies to a few, sometimes poorly penetrating, vital dyes. Another limitation of fluorescence microscopy is the fact that it only shows what has been fluorescently labelled; other structures remain (literally) in the dark. Structures that cannot be labeled simply cannot be visualized. It is therefore desirable to include other modalities in a light sheet instrument. By using the brightfield illumination that is typically present in a light sheet microscope, other microscopy techniques such as optical projection tomography (OPT) have been demonstrated [42]. The complementary data provides valuable insight into the state and stage of the sample.

Ideally, one would like to watch the development of a single embryo and have access to all the individual tissues, cellular compartments, and so on. Unfortunately, we currently cannot image more than three or four fluorescent colors simultaneously in a single sample due to the strong overlap of the emission spectra. Spectral detection with nanometer precision has been used to unmix several components of the full spectrum and distinguish many colors [43]. In the future, one can expect labeling and imaging techniques that offer a variaty of modalities to extract as much information out of a single sample as possible.

7.11 Outlook

7.11.1 Big Data

Light sheet microscopes can record images with high spatial and temporal resolution. Consequently, the rate and amount of data generated is about three orders of magnitude higher than in conventional confocal microscopes, often running into several terabytes for a single long-term imaging experiment [6]. Setups with multiple fast, high-resolution cameras [6–8, 27] may provide quick multiview acquisition and important new information, but several-folds more data are produced. Therefore, in such setups, the number of experiments is

limited by the available storage and/or transfer speed, preventing statistical analysis of image data necessary for quantitative biology. The issue of long-term storage can be tackled by data compression [8]; however, data processing, visualization, and analysis remain a challenge. As a consequence, there is a need to process, condense, and analyze light sheet microscopy data in real time.

Typical image stacks of organically shaped biological samples are cuboidal and therefore contain a lot of pixels with no information in the corners of the dataset. One way to efficiently reduce the amount of data is to crop the images as they come from the camera or, even better, selectively acquire regions of the sample where signal is expected and mask the rest. An even more efficient approach is to utilize the shape of the sample to create projections such as radial projections for the spherical early zebrafish embryos [6], cylindrical projections for Drosophila embryos [7], and other surface projections for arbitrary shaped objects [44]. These methods transform the 3D image data into 2D projections, thereby drastically reducing the amount of data while extracting maximum information from it on the fly and providing a novel way of visualizing and analyzing the data.

7.11.2 Smart Microscope: Imaging Concept of the Future

The concept of a smart microscope advocates that the microscope should decide how to best image the sample, given the experimenter's needs. It incorporates the idea of adaptive image acquisition: reading out only the relevant pixels to reduce the data stream, choosing the ROI based on prior knowledge, and identification of cellular events while imaging to adapt the FOV accordingly. Such a learning-based approach will make imaging and interpreting data much easier and comprehensible [45].

Sample health is one of the most crucial factors, as the reliability of the finding depends heavily on it. Hence, microscopes today are designed around their application, an idea aptly illustrated by the various implementations of light sheet microscopy. Ideally, samples are kept in their most natural environment and undisturbed while imaging. Noncontact imaging methods such as remote focusing using motorized or electrically tunable lenses [29] provide the best imaging conditions for keeping the sample immobile or freely swimming as need be, eliminating the need to embed sample in a stiff agarose gel. As these approaches also provide high imaging speeds, imaging of several samples in parallel becomes possible.

7.11.3 High-Throughput Imaging

Developmental processes are complex and vary significantly within a population. Obtaining a quantitative understanding of this variability and how it is dealt with to develop each embryo into a healthy individual is an important question. While it is possible to have a high sample count in other biological studies, imaging of developmental processes has so far been limited to a few samples only, owing to the exceedingly large amount of time and processing power required to perform each imaging experiment. As shown in this chapter, by using light sheet illumination instead of conventional point scanning, imaging speed increases

drastically, making light sheet microscopy the preferred method for *in vivo* imaging of developmental processes. With high-speed cameras, SPIM and its advanced implementations can, in fact, acquire 2D images and even 3D volumes at a rate much faster than most biological processes. Therefore, imaging several samples would be a way to utilize this time to increase experimental throughput.

Most industrial drug screens are limited to single cells due to the need for testing thousands of compounds, slow imaging speeds, and data handling issues. Genetic screens, on the other hand, are usually performed in research labs and involve a lot of manual labor, especially for injecting drugs or plasmids prior to screening. A light sheet microscopy-based high-throughput imaging platform will expedite the entire process and take drug and genetic screening to the next level with rapid high-resolution imaging of many cells, spheroids, and small embryos such as zebrafish exposed to different compounds.

Thus, a combination of the above-mentioned features will prevent us from drowning in data, yet capturing all relevant aspects of biological processes, possibly in a high-throughput fashion. Light sheet microscopy has the potential to address these current challenges and facilitate systematic and noninvasive quantitative biology.

7.12 Summary

Light sheet microscopy is a surprisingly simple yet very potent technology. The large collection of implementations demonstrates its power, versatility, and simplicity. The main advantages of low phototoxicity and high speed offer numerous applications that are simply out of reach of conventional fluorescence microscopy techniques. In the long run, light sheet techniques will benefit from the affordability and the ease of customization: the microscope can be built "around the sample" and may thereby offer the best imaging conditions and performance for many novel and demanding applications. In some cases, however, it may be difficult to implement the two-way access for illumination and detection optics. Single-lens solutions may then prove to be superior, particularly for conventional sample preparations. In the future, we will see numerous new applications, even in novel model organisms. One thing is for sure: we have come closer to noninvasive imaging of fragile biological samples, and this may already be the key to new discoveries.

References

1 Siedentopf, H. and Zsigmondy, R. (1902) Uber sichtbarmachung und größenbestimmung ultramikoskopischer teilchen, mit besonderer anwendung auf goldrubingläser. *Ann. Phys.*, **315** (1), 1–39.
2 Tsien, R.Y. (2010) Nobel lecture: constructing and exploiting the fluorescent protein paintbox. *Integr. Biol.*, **2** (2-3), 77–93.
3 Voie, A.H., Burns, D.H., and Spelman, F.A. (1993) Orthogonal-plane fluorescence optical sectioning: three-dimensional imaging of macroscopic biological specimens. *J. Microsc.*, **170** (3), 229–236.

4 Huisken, J., Swoger, J., Del Bene, F., Wittbrodt, J., and Stelzer, E.H.K. (2004) Optical sectioning deep inside live embryos by selective plane illumination microscopy. *Science*, **305** (5686), 1007–1009.
5 Keller, P.J., Schmidt, A.D., Wittbrodt, J., and Stelzer, E.H.K. (2008) Reconstruction of zebrafish early embryonic development by scanned light sheet microscopy. *Science*, **322** (5904), 1065–1069.
6 Schmid, B., Shah, G., Scherf, N., Weber, M., Thierbach, K., Campos, C.P., Roeder, I., Aanstad, P., and Huisken, J. (2013) High-speed panoramic light-sheet microscopy reveals global endodermal cell dynamics. *Nat. Commun.*, **4**, 2207.
7 Krzic, U., Gunther, S., Saunders, T.E., Streichan, S.J., and Hufnagel, L. (2012) Multiview light-sheet microscope for rapid in toto imaging. *Nat. Methods*, **9** (7), 730–733.
8 Tomer, R., Khairy, K., Amat, F., and Keller, P.J. (2012) Quantitative high-speed imaging of entire developing embryos with simultaneous multiview light-sheet microscopy. *Nat. Methods*, **9** (7), 755–763.
9 Wu, Y., Wawrzusin, P., Senseney, J., Fischer, R.S., Christensen, R., Santella, A., York, A.G., Winter, P.W., Waterman, C.M., Bao, Z., Colón-Ramos, D.A., McAuliffe, M., and Shroff, H. (2013) Spatially isotropic four-dimensional imaging with dual-view plane illumination microscopy. *Nat. Biotechnol.*, **31** (11), 1032–1038.
10 Lorenzo, C., Frongia, C., Jorand, R., Fehrenbach, J., Weiss, P., Maandhui, A., Gay, G., Ducommun, B., and Lobjois, V. (2011) Live cell division dynamics monitoring in 3D large spheroid tumor models using light sheet microscopy. *Cell Div.*, **6** (1), 22.
11 Ritter, J.G., Spille, J.H., Kaminski, T., and Kubitscheck, U. (2010) A cylindrical zoom lens unit for adjustable optical sectioning in light sheet microscopy. *Biomed. Opt. Express*, **2** (1), 185–193.
12 Planchon, T.A., Gao, L., Milkie, D.E., Davidson, M.W., Galbraith, J.A., Galbraith, C.G., and Betzig, E. (2011) Rapid three-dimensional isotropic imaging of living cells using Bessel beam plane illumination. *Nat. Methods*, **8** (5), 417–423.
13 Kumar, A., Wu, Y., Christensen, R., Chandris, P., Gandler, W., McCreedy, E., Bokinsky, A., Colón-Ramos, D.A., Bao, Z., McAuliffe, M., Rondeau, G., and Shroff, H. (2014) Dual-view plane illumination microscopy for rapid and spatially isotropic imaging. *Nat. Protoc.*, **9** (11), 2555–2573.
14 Dodt, H.U., Leischner, U., Schierloh, A., Jährling, N., Mauch, C.P., Deininger, K., Deussing, J.M., Eder, M., Zieglgänsberger, W., and Becker, K. (2007) Ultramicroscopy: three-dimensional visualization of neuronal networks in the whole mouse brain. *Nat. Methods*, **4** (4), 331–336.
15 Mickoleit, M., Schmid, B., Weber, M., Fahrbach, F.O., Hombach, S., Reischauer, S., and Huisken, J. (2014) High-resolution reconstruction of the beating zebrafish heart. *Nat. Methods*, **11** (9), 919–922.
16 Trivedi, V., Truong, T.V., Trinh, L.A., Holland, D.B., Liebling, M., and Fraser, S.E. (2015) Dynamic structure and protein expression of the live embryonic heart captured by 2-photon light sheet microscopy and retrospective registration. *Biomed. Opt. Express*, **6** (6), 2056–2066.

17 Maizel, A., von Wangenheim, D., Federici, F., Haseloff, J., and Stelzer, E.H.K. (2011) High-resolution live imaging of plant growth in near physiological bright conditions using light sheet fluorescence microscopy. *Plant J.*, **68** (2), 377–385.
18 Scherz, P.J., Huisken, J., Sahai-Hernandez, P., and Stainier, D.Y.R. (2008) High-speed imaging of developing heart valves reveals interplay of morphogenesis and function. *Development*, **135** (6), 1179–1187.
19 Swoger, J., Verveer, P., Greger, K., Huisken, J., and Stelzer, E.H.K. (2007) Multi-view image fusion improves resolution in three-dimensional microscopy. *Opt. Express*, **15** (13), 8029–8042.
20 Verveer, P.J., Swoger, J., Pampaloni, F., Greger, K., Marcello, M., and Stelzer, E.H.K. (2007) High-resolution three-dimensional imaging of large specimens with light sheet-based microscopy. *Nat. Methods*, **4** (4), 311–313.
21 Preibisch, S., Amat, F., Stamataki, E., Sarov, M., Singer, R.H., Myers, E., and Tomancak, P. (2014) Efficient Bayesian-based multiview deconvolution. *Nat. Methods*, **11** (6), 645–648.
22 Schmid, B. and Huisken, J. (2015) Real-time multi-view deconvolution. *Bioinformatics*, **31** (20), 3398–3400.
23 Truong, T.V., Supatto, W., Koos, D.S., Choi, J.M., and Fraser, S.E. (2011) Deep and fast live imaging with two-photon scanned light-sheet microscopy. *Nat. Methods*, **8** (9), 757–760.
24 Fahrbach, F.O. and Rohrbach, A. (2010) A line scanned light-sheet microscope with phase shaped self-reconstructing beams. *Opt. Express*, **18** (23), 24 229–24 244.
25 Breuninger, T., Greger, K., and Stelzer, E.H.K. (2007) Lateral modulation boosts image quality in single plane illumination fluorescence microscopy. *Opt. Lett.*, **32** (13), 1938–1940.
26 Huisken, J. and Stainier, D.Y.R. (2007) Even fluorescence excitation by multidirectional selective plane illumination microscopy (mSPIM). *Opt. Lett.*, **32** (17), 2608–2610.
27 Chhetri, R.K., Amat, F., Wan, Y., Höckendorf, B., Lemon, W.C., and Keller, P.J. (2015) Whole-animal functional and developmental imaging with isotropic spatial resolution. *Nat. Methods*, **12** (12), 1171–1178.
28 Holekamp, T.F., Turaga, D., and Holy, T.E. (2008) Fast three-dimensional fluorescence imaging of activity in neural populations by objective-coupled planar illumination microscopy. *Neuron*, **57** (5), 661–672.
29 Fahrbach, F.O., Gurchenkov, V., Alessandri, K., Nassoy, P., and Rohrbach, A. (2013) Light-sheet microscopy in thick media using scanned Bessel beams and two-photon fluorescence excitation. *Opt. Express*, **21** (11), 13 824–13 839.
30 Vladimirov, N., Mu, Y., Kawashima, T., Bennett, D.V., Yang, C.T., Looger, L.L., Keller, P.J., Freeman, J., and Ahrens, M.B. (2014) Light-sheet functional imaging in fictively behaving zebrafish. *Nat. Methods*, **11** (9), 883–884.
31 Ritter, J.G., Veith, R., Siebrasse, J.P., and Kubitscheck, U. (2008) High-contrast single-particle tracking by selective focal plane illumination microscopy. *Opt. Express*, **16** (10), 7142–7152.

32 Gebhardt, J.C.M., Suter, D.M., Roy, R., Zhao, Z.W., Chapman, A.R., Basu, S., Maniatis, T., and Xie, X.S. (2013) Single-molecule imaging of transcription factor binding to DNA in live mammalian cells. *Nat. Methods*, **10** (5), 421–426.

33 Hama, H., Hioki, H., Namiki, K., Hoshida, T., Kurokawa, H., Ishidate, F., Kaneko, T., Akagi, T., Saito, T., Saido, T., and Miyawaki, A. (2015) ScaleS: an optical clearing palette for biological imaging. *Nat. Neurosci.*, **18** (10), 1518–1529.

34 Chung, K. and Deisseroth, K. (2013) CLARITY for mapping the nervous system. *Nat. Methods*, **10** (6), 508–513.

35 Bouchard, M.B., Voleti, V., Mendes, C.S., Lacefield, C., Grueber, W.B., Mann, R.S., Bruno, R.M., and Hillman, E.M.C. (2015) Swept confocally-aligned planar excitation (SCAPE) microscopy for high speed volumetric imaging of behaving organisms. *Nat. Photonics*, **9** (2), 113–119.

36 Reynaud, E.G., Krzic, U., Greger, K., and Stelzer, E.H.K. (2008) Light sheet-based fluorescence microscopy: more dimensions, more photons, and less photodamage. *HFSP J.*, **2** (5), 266–275.

37 Kaufmann, A., Mickoleit, M., Weber, M., and Huisken, J. (2012) Multilayer mounting enables long-term imaging of zebrafish development in a light sheet microscope. *Development*, **139** (17), 3242–3247.

38 Pampaloni, F., Berge, U., Marmaras, A., Horvath, P., Kroschewski, R., and Stelzer, E.H.K. (2014) Tissue-culture light sheet fluorescence microscopy (TC-LSFM) allows long-term imaging of three-dimensional cell cultures under controlled conditions. *Integr. Biol.*, **6** (10), 988–998.

39 Baumgart, E. and Kubitscheck, U. (2012) Scanned light sheet microscopy with confocal slit detection. *Opt. Express*, **20** (19), 21 805–21 814.

40 Fahrbach, F.O. and Rohrbach, A. (2012) Propagation stability of self-reconstructing Bessel beams enables contrast-enhanced imaging in thick media. *Nat. Commun.*, **3**, 632.

41 Chen, B.C., Legant, W.R., Wang, K., Shao, L., Milkie, D.E., Davidson, M.W., Janetopoulos, C., Wu, X.S., Hammer, J.A. III, Liu, Z., English, B.P., Mimori-Kiyosue, Y., Romero, D.P., Ritter, A.T., Lippincott-Schwartz, J., Fritz-Laylin, L., Mullins, R.D., Mitchell, D.M., Bembenek, J.N., Reymann, A.C., Böhme, R., Grill, S.W., Wang, J.T., Seydoux, G., Tulu, U.S., Kiehart, D.P., and Betzig, E. (2014) Lattice light-sheet microscopy: imaging molecules to embryos at high spatiotemporal resolution. *Science*, **346** (6208), 1257 998.

42 Bassi, A., Schmid, B., and Huisken, J. (2015) Optical tomography complements light sheet microscopy for in toto imaging of zebrafish development. *Development*, **142** (5), 1016–1020.

43 Jahr, W., Schmid, B., Schmied, C., Fahrbach, F.O., and Huisken, J. (2015) Hyperspectral light sheet microscopy. *Nat. Commun.*, **6**, 7990.

44 Heemskerk, I. and Streichan, S.J. (2015) Tissue cartography: compressing bio-image data by dimensional reduction. *Nat. Methods*, **12** (12), 1139–1142.

45 Scherf, N. and Huisken, J. (2015) The smart and gentle microscope. *Nat. Biotechnol.*, **33** (8), 815–818.